nature genetics

Bmi1 is expressed *in vivo* in intestinal stem cells

Eugenio Sangiorgi & Mario R Capecchi

Bmi1 **plays an essential part in the self-renewal of hematopoietic and neural stem cells. To investigate its role in other adult stem cell populations, we generated a mouse expressing a tamoxifen-inducible Cre from the** ***Bmi1*** **locus. We found that** ***Bmi1*** **is expressed in discrete cells located near the bottom of crypts in the small intestine, predominantly four cells above the base of the crypt (+4 position). Over time, these cells proliferate, expand, self-renew and give rise to all the differentiated cell lineages of the small intestine epithelium. The induction of a stable form of β-catenin in these cells was sufficient to rapidly generate adenomas. Moreover, ablation of** ***Bmi1***$^{+}$ **cells using a** ***Rosa26*** **conditional allele, expressing diphtheria toxin, led to crypt loss. These experiments identify** ***Bmi1*** **as an intestinal stem cell marker** ***in vivo.*** **Unexpectedly, the distribution of** ***Bmi1*****-expressing stem cells along the length of the small intestine suggested that mammals use more than one molecularly distinguishable adult stem cell subpopulation to maintain organ homeostasis.**

Adult somatic stem cells are defined by two major properties: the ability to generate more stem cells (self-renewal) and the ability to generate differentiated cell lineages[1]. To establish the presence of these two properties, the gold standard is to assess both of them *in vivo* and *in vitro*[2]. Several studies have shown *in vitro* that many tissues carry cells capable of self-renewal and of giving rise to differentiated cell types. However, few experiments have clearly established *in vivo* self-renewal and multipotency of these cells over time[3,4].

To address this, we established a genetic fate-mapping system for stem cell populations *in vivo*. We chose as our target locus *Bmi1*, a gene already known to be involved in the self-renewal of neuronal, hematopoietic and leukemic cells[5–7]. *Bmi1* was first identified in a mouse proviral insertion screen for lymphomagenesis[8]. It is part of the Polycomb group gene family, and specifically a member of polycomb-repressing complex 1 (PRC1). PRC1 has an essential role in maintaining chromatin silencing[9,10]. *Bmi1*$^{-/-}$ mice die before or near weaning from a defect in self-renewal of hematopoietic stem cells[11,12]. Our hypothesis was that PRC1 might be part of a general mechanism for maintaining self-renewal in various adult stem cell populations.

We inserted a construct encoding a internal ribosome entry site (IRES)–Cre–estrogen receptor binding domain fusion (*IRES-Cre-ER*) into the 3′ untranslated region of *Bmi1* (**Supplementary Fig. 1** online), such that expression of Cre recombinase in *Bmi1*-expressing cells was under the temporal control of tamoxifen without interfering with *Bmi1* function[13,14]. We crossed mice carrying this allele with a reporter mouse in which Cre activity induces expression of β-galactosidase (LacZ) or yellow fluorescent protein (YFP) from the ubiquitously active *Rosa26* locus[15]. Thus, cells expressing *Bmi1* and their progeny, marked at the time of tamoxifen treatment, were permanently labeled. Using this approach, we found that the small intestine was one tissue that showed a prominent *Bmi1*$^{+}$ lineage.

The small intestine is one of the best models for studying adult stem cells *in vivo*[16]. A crypt and villus represent the fundamental repetitive unit. The crypt is the proliferative compartment, composed of 250–300 cells in constant, active proliferation, and generates all the cells required to renew the entire intestinal epithelium in 2–5 d in mice[17,18]. Intestinal stem cells (ISCs) have been proposed to be located just above Paneth cells[19], or in a permissive microenvironment within the first four to five cell positions from the bottom of the crypt, with some ISCs interspersed among Paneth cells[20].

To establish the *Bmi1* expression domain in the intestine, we took advantage of our genetic fate-mapping system. To identify cells initially labeled by *Bmi1* expression, it is important to analyze expression of the LacZ reporter as early as possible after tamoxifen injection. The primary location of ISCs—between Paneth cells[21] or above them[19]—has been a matter of some debate. To assess the position of *Bmi1*-expressing cells early after tamoxifen induction, we harvested small intestines from *Bmi1*$^{Cre\text{-}ER/+}$;*Rosa26*$^{LacZ/+}$ mice at different time points, stained them for LacZ activity and sectioned them.

To score the location of single Bmi1^{+} cells, we used the following criteria: only a single Bmi1^{+} cell, based on serial adjacent sections, had to be present in a crypt that was longitudinally cut, and Paneth cells were identified morphologically with Nomarski optics. A total of 91 crypts were scored indisputably as showing only one LacZ^{+} cell: 86 of these cells were located above the Paneth cells in a position approximately +4, +5 from the base of the crypt (**Fig. 1a–h**), and 5 were located intermingled among Paneth cells. In many crypts, there was more than one labeled cell (**Fig. 1c**,**d**,**f**). On the basis of their positions along the crypt axis, multiple labeled cells could represent multiple ISCs (**Fig. 1c**,**f**; yellow arrowheads). However, cells in the crypt are rapidly dividing and migrating, so it is plausible that in some

Howard Hughes Medical Institute and Department of Human Genetics, University of Utah School of Medicine, Salt Lake City, Utah 84112, USA. Correspondence should be addressed to M.R.C. (mario.capecchi@genetics.utah.edu).

Received 12 February; accepted 2 April; published online 8 June 2008; doi:10.1038/ng.165

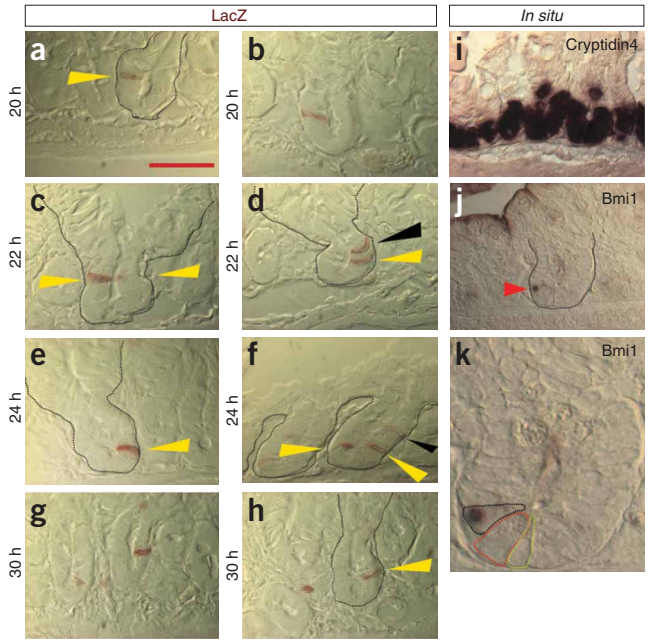

Figure 1 Early *Bmi1*$^{+}$ lineage detection. (**a**–**h**) *Bmi1*$^{CreER/+}$;*Rosa26*$^{LacZ/+}$ mice were injected with tamoxifen, and after 20, 22, 24 or 30 h, the duodenum and the jejunum were stained in whole mount for LacZ and then longitudinally sectioned. Crypts cut along their major axis containing only a single cell labeled were analyzed. **a**–**c**,**e**,**g**,**h** show representative pictures of crypts with a single LacZ^{+} cell present at position +4, +5 (yellow arrowheads). **c**,**d**,**f** show representative pictures of crypts in which more than one labeled cell is present. In **c**, the tip of the second cell is barely visible. Black arrowheads in **d**,**f** indicate cells that have already started migrating upward. (**i**–**k**) *In situ* hybridization of the small intestine with a control probe (**i**) labeling the Paneth cells and with a *Bmi1* probe (**j**). *Bmi1*mRNA is present only at the bottom of the crypts in cells located above Paneth cells (red arrowhead). Digital magnification (2.5×) (**k**) of the crypt highlighted in **j** shows *Bmi1* in a cell (black dashed line) located above a Paneth cell (red dashed line); next to the Paneth cell a crypt base columnar cell is visible (yellow dashed line). All photographs (except **k**) were captured at the same magnification. Scale bar, 50 μm.

crypts, multiple Bmi1^{+} cells, when located further up in the crypt (**Fig. 1d**,**f**; black arrowhead), represent the progeny of the early Bmi1 lineage that had already started migrating and differentiating upward toward the villi. We confirmed the expression of *Bmi1* in these cells by *in situ* hybridization, showing that the *Bmi1* transcript is present only in cells located at the bottom of the crypt (**Fig. 1i**–**k**), above and occasionally among the Paneth cells.

To evaluate the repopulation kinetics of the crypt cells derived from Bmi1^{+} parents, we analyzed the small intestines of *Bmi1*$^{Cre\text{-}ER/+}$;*Rosa26*$^{LacZ/+}$ mice from day 2 to day 30 after tamoxifen induction, analyzing and following crypts on serial adjacent sections. Crypts with LacZ^{+} cells presented a large variation in the number of stained cells. From day 2 to day 30, there was a continual increase in the number of cells labeled per crypt (**Fig. 2a**–**l**). Over time, the number of crypts that were completely stained progressively increased, but there were still crypts at 13, 19, 24 and 30 d showing patches or halves with unlabeled cells (**Fig. 2h**–**l**). We counted the number of crypts completely labeled at different time points (**Fig. 2m**), and by 24–30 d after tamoxifen, all the crypts were half or fully labeled. At 24 d, 21% (35/164) of crypts were half labeled and the others were fully labeled. One technical explanation for these observations is that a single tamoxifen injection might not label all of the stem cells present in a crypt. It is also possible that, even though multiple stem cells are labeled at the same time, not all of them are synchronously replicating and renewing. There is no easy way to discriminate between these two hypotheses, and both mechanisms could contribute to our observations.

We observed that the *Bmi1*$^{+}$ lineage, in whole-mount staining and on sections, was present in approximately 10% of the crypts throughout the first 10 cm of the small intestine, with a descending gradient of labeled crypts (**Fig. 3a**–**e**). Beyond 20 cm from the pylorus, there was no visible LacZ staining (**Fig. 3a**–**e**). As a control, we harvested mice of the same genotype that were not exposed to tamoxifen at 2, 3, 4 and 6 months of age. We did not observe any LacZ-staining cells either in whole mounts or on sections of small intestines from any of these

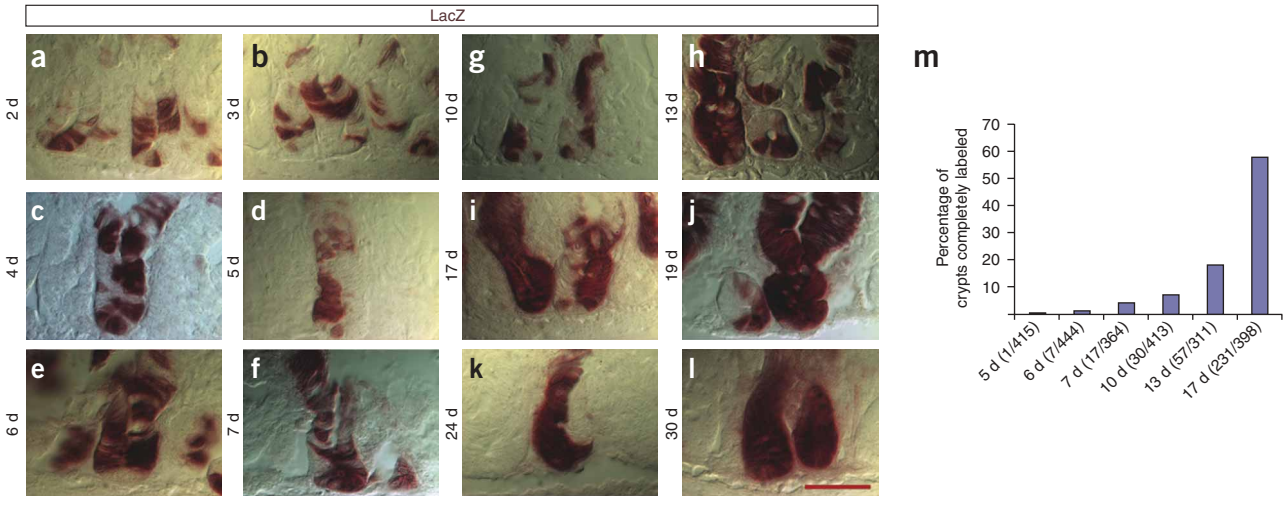

Figure 2 Repopulation kinetics of the *Bmi1*$^{+}$ lineage. (**a**–**l**) Small intestines were harvested from *Bmi1*$^{CreER/+}$;*Rosa26*$^{LacZ/+}$ mice at different time points from day 2 to day 30. We analyzed and followed crypts on serial adjacent sections and observed that, even after 19, 24 and 30 d, many crypts were half filled by the *Bmi1*$^{+}$ lineage. (**m**) To evaluate the repopulation kinetics, fully labeled crypts were counted at different time points after tamoxifen injection. All the pictures were captured at the same magnification. Scale bar, 50 μm.

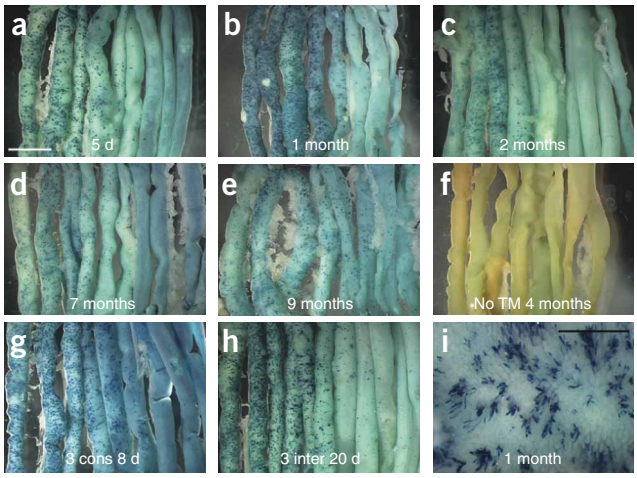

Figure 3 *Bmi1*$^{+}$ lineage analysis in the small intestine. (**a**–**e**) After a single injection of tamoxifen, the *Bmi1*$^{+}$ lineage is present from day 5 up to 9 months. The *Bmi1*$^{+}$ lineage in the whole intestine is more abundant in the duodenum (top left corner) and in the first part of the jejunum, with almost no staining in the ileum (bottom right corner). After 1 month, there is an apparent modest progressive reduction in the number of labeled crypts. (**f**) The intestine of a 4-month-old *Bmi1*$^{CreER/+}$;*Rosa26*$^{LacZ/+}$ mouse does not show any LacZ staining without tamoxifen induction. (**g**,**h**) Two *Bmi1*$^{CreER/+}$;*Rosa26*$^{LacZ/+}$ mice received tamoxifen injection for 3 consecutive d (**g**), whereas two other mice with the same genotype were treated three times at 5-d intervals (**h**). Five days after the last injection, the intestines were harvested and stained for LacZ. (**i**) Intestinal mucosa of a *Bmi1*$^{CreER/+}$;*Rosa26*$^{LacZ/+}$ mouse 4 months after a single tamoxifen injection. The *Bmi1*$^{+}$ lineage is visible on villi as a 'line' of cells coming from the crypt. White scale bar, 5 mm; black scale bar, 1 mm.

control animals (**Fig. 3f**). These results demonstrate that *Bmi1-Cre-ER* is strictly dependent on tamoxifen for its function.

We asked whether the gradient of Bmi1^{+} expression could be related to tamoxifen induction rather than representing the actual expression domain of *Bmi1*. The dosage of tamoxifen used was the highest concentration that has been reported to give maximum staining[13]. Nonetheless, it is possible that not all the cells expressing Cre-ER interacted with the drug. Alternatively, mosaic expression could have been related to *Bmi1* expression itself. If *Bmi1* is expressed only during a specific phase of the cell cycle, in a cell population that is slow cycling, a single injection might detect only a few of the potential *Bmi1*-expressing cells.

To address these two possibilities, we used two different tamoxifen injection schedules. We injected two *Bmi1*$^{Cre\text{-}ER/+}$;*Rosa26*$^{LacZ/+}$ mice for 3 consecutive days to attempt to saturate all the Cre-ER molecules and obtain maximum recombination. We treated two other mice with the same genotype with tamoxifen at 5-d intervals for a total of three injections in order to try to label *Bmi1*-expressing cells with potentially different cell cycles. In both experiments, 5 d after the last injection, we harvested the small intestines and stained them for LacZ. However, in both multiple-injection protocols, we did not observe any marked increase in the number of crypts labeled compared to that in mice receiving a single injection of tamoxifen (**Fig. 3g**,**h**). This expression pattern was further confirmed by RNA *in situ* hybridization. The first 10 cm of the small intestine showed *Bmi1* expression at the bottom of some crypts, with a descending gradient of expression thereafter (**Supplementary Fig. 2** online).

One month after tamoxifen injection, the *Bmi1*$^{+}$ lineage inside the lumen of the small intestine was clearly visible, starting from a crypt and radiating as a 'column' of cells all the way to the top of the adjacent villus (**Fig. 3i**). These findings confirmed previous reports showing that a single crypt contributes only one or two 'rows' of cells to the adjacent villi[22].

To analyze the state of *Bmi1*-expressing cells, we examined the lineage with differentiated cell markers for enteroendocrine cells, Paneth cells and goblet cells. We noticed that, after 5 d, some crypts still had only one or two cells labeled by the *Bmi1* live reporter, indicating that *Bmi1*-expressing cells are slow cycling or have a different renewing cycle. Using antibodies for differentiated cell markers, alone or in combination, whenever we analyzed crypts

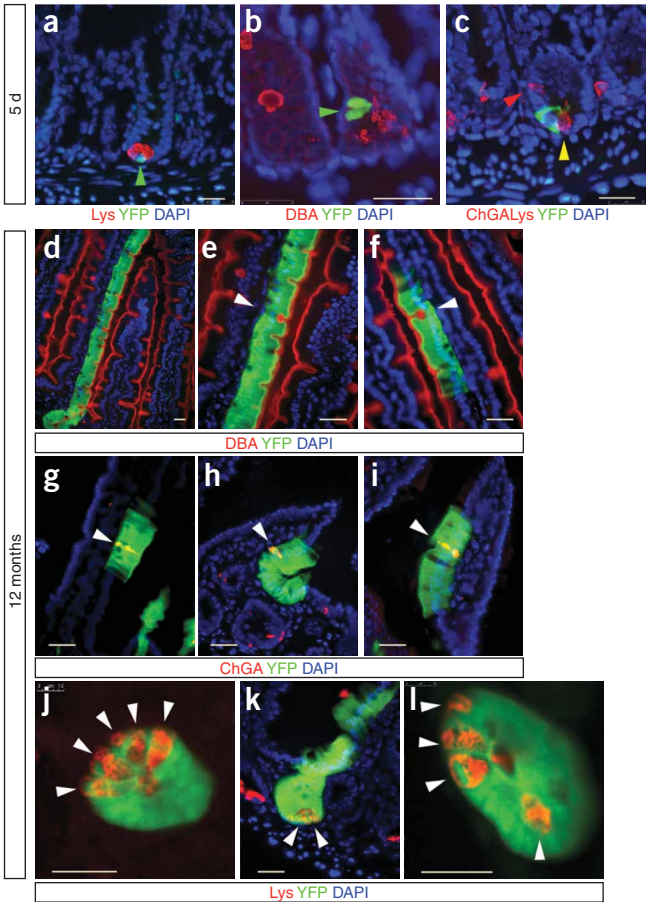

Figure 4 Assessment of *Bmi1*$^{+}$ lineage after 5 d and after 12 months to evaluate the colocalization with differentiated-cell markers. (**a**–**c**) Five days after tamoxifen injection, the *Bmi1*$^{+}$ lineage (YFP; green arrowheads) is present at the bottom of a crypt. The antibody to lysozyme (Lys) identifies Paneth cells (**a**). DBA stains Goblet cells (**b**). (**c**) Intestinal section showing staining with YFP, indicating the *Bmi1*$^{+}$ lineage; chromogranin A (ChGA), labeling enteroendocrine cells (red arrowhead); and lysozyme antibody, indicating Paneth cells (yellow arrowhead). (**d**–**l**) After 12 months, the *Bmi1*$^{+}$ lineage is present in all differentiated intestinal cell types. In **d**, the Bmi1 lineage is expanding from a crypt all the way to the top of an adjacent villus; several goblet cells (DBA^{+}) are present in the Bmi1 lineage. **e** is a 2× magnification of **d**. The white arrowhead indicates a goblet cell. Another Bmi1^{+} goblet cell is shown in **f** (white arrowhead). **g**–**i** show three examples of enteroendocrine cells (ChGA^{+}; white arrowheads) within the Bmi1 lineage. Two transverse (**j**,**l**) and one longitudinal (**k**) section of Bmi1^{+} crypts, showing that Paneth cells (Lys^{+}; white arrowheads) are present in the Bmi1 lineage. Scale bars, 25 μm.

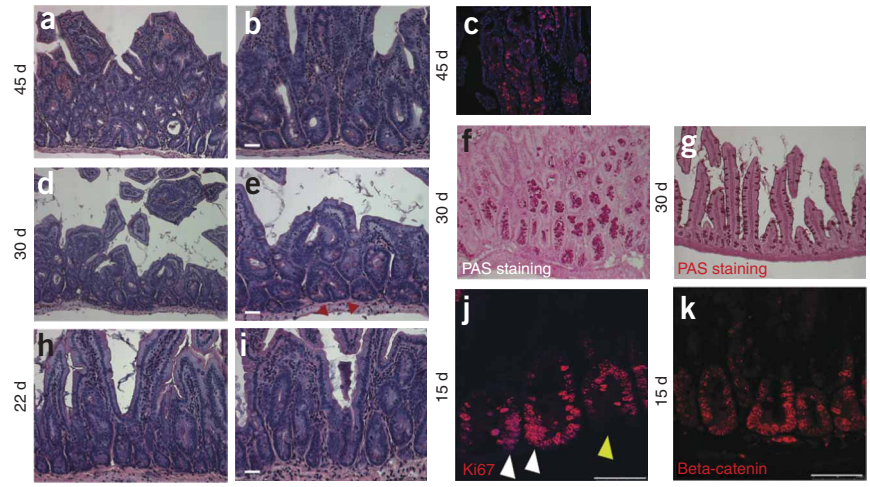

Figure 5 *Bmi1*$^{CreER/+}$;*Ctnnb1*$^{Ex3LoxP/+}$ cross. Forty-five days after tamoxifen injection, the duodenum and the jejunum contain multiple adenomas. (**a**,**b**) Low (**a**) and high (**b**) magnifications. (**c**) The adenomas were BrdU positive. (**d**,**e**) Low (**d**) and (**e**) high magnifications. At day 30, only a few adenomas are visible. In many areas with or without adenomas, many crypts were in fission (red arrowheads). (**f**,**g**) Many crypts showed numerous periodic acid–Schiff (PAS)-positive cells (Paneth and goblet cells) present (**f**), indicating an expansion of the secretory compartment compared to the wild-type intestine (**g**). (**h**,**i**) Low (**h**) and (**i**) high magnification. At day 22 only rare adenomas were visible. (**j**) After staining with Ki67, many crypts showed increased number of proliferating cells crowded at the position where ISCs are located (white arrowheads). The yellow arrowhead indicates an adjacent crypt showing the normal Ki67 staining. (**k**) β-catenin staining, showing ubiquitous expression. Scale bars: 25 μm (**b**,**e**,**i**); 50 μm (**j**,**k**).

containing only one or few YFP-positive cells, we found no cases of cells labeled by both YFP and any differentiated state marker (**Fig. 4a–c**). Each YFP$^+$ clone contained all differentiated cell types in the same proportions as in the YFP$^-$ clones.

Stem cells, unlike progenitor cells, are able to self-renew, and the most stringent test of self-renewal is the persistence of the lineage for the lifespan of a mouse. Examination of mouse small intestines harvested at 1, 2, 4, 6, 7, 8, 9 and 12 months after tamoxifen injection showed that the lineage was still present, although with an apparent modest reduction over time in the number of stained crypts (**Fig. 3b–e**). We analyzed intestinal sections of *Bmi1*$^{Cre-ER/+}$; *Rosa26*$^{YFP/+}$ mice at the same time points and invariably found that every crypt labeled projected a 'row' or two of cells to the top of an adjacent villus, and that the *Bmi1*$^+$ lineage was present in all the differentiated cell types (**Fig. 4d–l**). However, even in the duodenum, where the density of *Bmi1*-expressing ISCs was the highest, neither LacZ nor RNA *in situ* hybridization labeled stem cells in every crypt. These experiments imply that either there exist actively cycling ISCs in the duodenum that do not express *Bmi1*, or *Bmi1* is not constitutively expressed in ISCs, or both.

It has been proposed that some leukemias and solid tumors contain stem cells capable of self-renewal[23]. To investigate the role of *Bmi1*-labeled stem cells in the initiation of cancer, we crossed *Bmi1-Cre-ER* mice with a conditional β-catenin (Ex3-LoxP) stable expression allele[24]. Upon Cre recombination, the LoxP-flanked exon 3 of *Ctnnb1* (encoding β-catenin) is excised, and the resulting stabilized protein fails to undergo degradation and is able to activate transcription of target genes. Using a general small-intestine Cre driver that functions throughout mouse development, stable expression of β-catenin leads to the generation of multiple adenomas[24]. We tested whether adenomas would be generated by expression of the same β-catenin allele in *Bmi1*-expressing ISCs in adults. We injected compound-heterozygous *Bmi1*$^{Cre-ER/+}$; *Ctnnb1*$^{Ex3-LoxP/+}$ mice with tamoxifen after weaning. Three out of three mice showed signs of distress after approximately 30 d and died after 50 d. We examined the duodena of mice killed at regular intervals from 5 to 45 d after injection. Adenomas were present everywhere in the first part of the intestine at day 45 (**Fig. 5a–c**). The adenomas showed the expected morphology of adenomas in mouse, in which the proliferating cells grow inside an apparent normal epithelial layer generating crypt-like structures. Adenomas first started forming between days 22 and 30 (**Fig. 5d–i**). At day 15, in areas where adenomas had not yet developed, an increased number of crypts presented a crowded population of cells expressing Ki67 (a marker for proliferating cells). As expected, β-catenin nuclear staining was present everywhere (**Fig. 5j–k**).

To examine the consequences of ablating the candidate stem cells in the small intestine, we crossed the *Bmi1-Cre-ER* driver with a conditional allele encoding diphtheria toxin expressed from the *Rosa26* locus[25]. Double-heterozygous mice (*Bmi1*$^{Cre-ER/+}$; *Rosa26*$^{DTA/+}$) were viable and healthy. Upon administration of tamoxifen for 3 consecutive days after weaning, the mice died within 2–3 d, showing small intestines full of dead cells (data not shown). When given a single injection of tamoxifen, the mice survived, although their weight failed to increase for several weeks. The small intestines of singly injected mice were analyzed at 6, 11, 22, 30 and 60 d after injection ($n = 2$ for each time point). At all time points, several areas within the duodenum and jejunum were devoid of crypts and had been replaced by an unidentified cell population **Figure 6a–i**. In surrounding tissue, several crypts were in fission and branching, replacing the missing crypts. At 9 months and 15 months after single injection of tamoxifen, the mice had regained their weight to match that of uninjected controls. The small intestines of these mice appeared histologically normal, suggesting that surrounding surviving crypts are able to replace missing ones.

The search for markers identifying ISCs *in vivo* has been difficult. Twenty hours after tamoxifen injection, *Bmi1-Cre-ER* predominantly labels a discrete cell population present above Paneth cells at the +4 position from the base of the crypt. These cells are undifferentiated, proliferate, give rise to differentiated cells and self-renew over time. These properties are strictly required to identify any cell population as stem cells. Thus, we conclude that *Bmi1*-expressing cells represent one of the stem cell populations of the small intestine.

Very recently, other researchers identified *Lgr5*, encoding an orphan G protein–coupled receptor, as an ISC marker[26]. Notably, *Lgr5* predominantly labels ISCs at the base of the crypt, among Paneth cells, whereas *Bmi1* labels ISCs predominantly at the +4 position of the crypt. Based on the apparently more rapid entry of *Lgr5*-labeled cells, relative to *Bmi1*-labeled cells, into the proliferative state (that is, the more rapid expansion of the LacZ-labeled cells after tamoxifen induction)[26], it is tempting to speculate that these two markers label different states of ISCs: a more quiescent state (*Bmi1*) and a state more prone to enter proliferation (*Lgr5*). The fact that they are in different

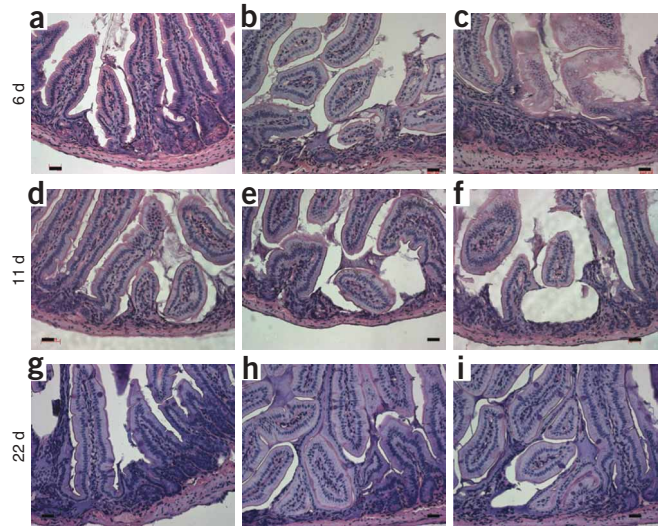

Figure 6 Intestinal stem cell ablation. After one injection of tamoxifen, *Bmi1*$^{CreER/+}$;*Rosa26*$^{DTA/+}$ mice were killed at different time points and their small intestine analyzed. (**a**–**i**) Representative pictures at 6, 11 and 22 d showing patches of intestinal mucosa disorganized and in disarray, without crypts. The ablation of the *Bmi1*$^{+}$ ISC lineage is responsible for the crypt loss. Scale bar, 50 μm.

stem cell niches suggests that these cells could potentially migrate from one niche to another.

It is difficult to evaluate the kinetics of repopulation of the crypts using a stem cell marker because all the stem cells in a crypt might not be labeled, different ISCs in the same crypt might enter lineage production at different times, or both. Our results do not contradict the existing data indicating that the whole crypt and villi are renewed in 2–5 d, but rather complement those data. Those data were generated using metabolic markers such as BrdU and [^{3}H]thymidine, which labels all proliferative cells (stem cells and intermediate progenitors) at the same time. In our experiment, the renewal of the whole crypt starts from individual cells, potentially in different cellular states (see above). In addition, different intermediate progenitors along the crypt have a different life span, and it may take longer to replace some than others.

The small intestine is not uniform with respect to function along its length, showing clearly defined differential absorption and secretion profiles as a function of position. The nonuniformity of the small intestine is also apparent from the nonuniform expression of many genes, including *Hox* genes, along its length. What may be surprising, however, is that this complexity is reflected at the level of its stem cell biology. *Bmi1*-expressing cells are present in a descending gradient, with many more crypts labeled in the duodenum and the first part of the jejunum and progressively fewer to none present in the ileum. The nonuniform distribution of *Bmi1*-expressing stem cells in the small intestine also suggests that more than one adult stem cell population may be present there. On the other hand, it could be argued that the very rapid turnover of this tissue (2–5 d in mouse) may impose a requirement for programming in some of the complexities of this tissue at a very early stage of its formation (through the existence of distinct adult stem cell populations along its length).

The observed pattern of *Bmi1* expression suggests that other genes in PRC1 may be expressed in other ISC populations. A candidate gene is *Mel18*. The Mel18 and Bmi1 proteins show a high degree of similarity, both in their function as transcription repressors and in their ability to bind to the same group of Polycomb proteins, but they could be sufficiently distinct to allow control of different differentiation programs[27].

Stable expression of β-catenin in the *Bmi1* expression domain sheds light on the mechanism of cancer formation in the small intestine. Two models for the histogenesis of colorectal cancer have been suggested: the stem cell–derived "bottom-up" model[28], and the "top-down" model, which theorizes that dysplastic cells located in the intracryptal region eventually spread down[29]. Our findings not only lend support to the bottom-up theory for the generation of adenomas, but also confirm that the expansion of stem cell clones can lead to increased migration and proliferation in the bottom of a crypt and then to crypt duplication.

Targeted cell ablation by diphtheria toxin showed that removal of stem cells in some crypts leads to their complete disruption. This suggests that Bmi1^{+} ISCs are crucial for crypt maintenance. Because not all crypts were affected, adjacent surviving crypts were able to compensate by generating new crypts.

In summary, we present here results showing that, *in vivo*, *Bmi1* is expressed in ISCs. The data include (i) pulse-chase fate mapping, unambiguously demonstrating the self-renewal capacity of Bmi1^{+} cells; (ii) colabeling of the progeny of Bmi1^{+} cells with differentiation markers to demonstrate pluripotency; (iii) induction of cancer in adult animals via stabilized β-catenin expression in these cells; and (iv) *Bmi1*$^{+}$-dependent cell-ablation experiments proving that *Bmi1*-expressing cells are required for crypt maintenance. Equally importantly, the results support our original hypothesis that self-renewal of adult stem cells may be controlled by PRC1, thereby allowing investigators to label and genetically manipulate adult stem cells *in vivo* through *Bmi1*. If the complexity that we observe in adult ISCs is intrinsic to these adult cells, then our observations also have important implications for the implementation of future stem cell-based therapies.

METHODS

Generation of *Bmi1*-IRES-*Cre-ER* mice. The *Bmi1*-IRES-*Cre-ER* allele was generated using standard cloning techniques, as described in **Supplementary Methods** online. The Cre-ERT construct was a gift from A. McMahon (Harvard University). Primer sequences are listed in **Supplementary Table 1** online. Mice heterozygous and homozygous for the *Bmi1*-IRES-*Cre-ER* allele are viable, fertile and manifest no detectable phenotype, even after tamoxifen injection. Tamoxifen (Sigma) was dissolved directly in corn oil (Sigma) at a final concentration of 20 mg/ml, and was injected intraperitoneally in adult mice between postnatal days 30 and 50 at a concentration of 9 mg per 40 g body weight. All studies and procedures involving animal subjects were approved by the University of Utah Institutional Animal Care and Use Committee and conducted strictly in accordance with the approved animal handling protocol.

Immunohistochemistry. All immunohistochemistry experiments were done using standard techniques. Antibody dilution and antigen retrieval are described in the **Supplementary Methods**. All the fluorescent images were captured using a Leica TCS SP5 laser-scanning confocal microscope.

Note: Supplementary information is available on the Nature Genetics website.

ACKNOWLEDGMENTS

We thank M. Taketo for providing the β-catenin mouse line; A. Sanchez-Alvarado, A. Boulet, L. Carroll, S. Covington, M. Hockin and K. Thomas for critical reading of the manuscript; and the other members of the Capecchi laboratory for sharing discussions and ideas. We gratefully acknowledge efforts by all of the members of our tissue culture and mouse facility, in particular S. Barnett, C. Lenz and J. Tomlin.

AUTHOR CONTRIBUTIONS

E.S. designed this study, performed the experiments and wrote the paper; M.R.C. designed this study and wrote the paper.

Published online at http://www.nature.com/naturegenetics/
Reprints and permissions information is available online at http://npg.nature.com/reprintsandpermissions/

1. Wagers, A.J. & Weissman, I.L. Plasticity of adult stem cells. *Cell* **116**, 639–648 (2004).
2. Seaberg, R.M. & van der Kooy, D. Stem and progenitor cells: the premature desertion of rigorous definitions. *Trends Neurosci.* **26**, 125–131 (2003).
3. Shackleton, M. *et al.* Generation of a functional mammary gland from a single stem cell. *Nature* **439**, 84–88 (2006).
4. Ahn, S. & Joyner, A.L. *In vivo* analysis of quiescent adult neural stem cells responding to Sonic hedgehog. *Nature* **437**, 894–897 (2005).
5. Lessard, J. & Sauvageau, G. Bmi-1 determines the proliferative capacity of normal and leukaemic stem cells. *Nature* **423**, 255–260 (2003).
6. Leung, C. *et al.* Bmi1 is essential for cerebellar development and is overexpressed in human medulloblastomas. *Nature* **428**, 337–341 (2004).
7. Molofsky, A.V. *et al.* Bmi-1 dependence distinguishes neural stem cell self-renewal from progenitor proliferation. *Nature* **425**, 962–967 (2003).
8. van Lohuizen, M. *et al.* Identification of cooperating oncogenes in Eμ-myc transgenic mice by provirus tagging. *Cell* **65**, 737–752 (1991).
9. Valk-Lingbeek, M.E. & Bruggeman, S.W.M. & van Lohuizen, M. Stem cells and cancer: the Polycomb connection. *Cell* **118**, 409–418 (2004).
10. Widschwendter, M. *et al.* Epigenetic stem cell signature in cancer. *Nat. Genet.* **39**, 157–158 (2007).
11. van der Lugt, N.M. *et al.* Posterior transformation, neurological abnormalities, and severe hematopoietic defects in mice with a targeted deletion of the bmi-1 proto-oncogene. *Genes Dev.* **8**, 757–769 (1994).
12. Park, I.K. *et al.* Bmi-1 is required for maintenance of adult self-renewing haematopoietic stem cells. *Nature* **423**, 302–305 (2003).
13. Hayashi, S. & McMahon, A.P. Efficient recombination in diverse tissues by a tamoxifen-inducible form of Cre: a tool for temporally regulated gene activation/inactivation in the mouse. *Dev. Biol.* **244**, 305–318 (2002).
14. Indra, A.K. *et al.* Temporally-controlled site-specific mutagenesis in the basal layer of the epidermis: comparison of the recombinase activity of the tamoxifen- inducible Cre-ER(T) and Cre-ER(T2) recombinases. *Nucleic Acids Res.* **27**, 4324–4327 (1999).
15. Soriano, P. Generalized lacZ expression with the *ROSA26* Cre reporter strain. *Nat. Genet.* **21**, 70–71 (1999).
16. Potten, C.S. Radiation, the ideal cytotoxic agent for studying the cell biology of tissues such as the small intestine. *Radiat. Res.* **161**, 123–136 (2004).
17. Bjerknes, M. & Cheng, H. Clonal analysis of mouse intestinal epithelial progenitors. *Gastroenterology* **116**, 7–14 (1999).
18. Wong, M.H., Stappenbeck, T.S. & Gordon, J.I. Living and commuting in intestinal crypts. *Gastroenterology* **116**, 208–210 (1999).
19. Potten, C.S., Owen, G. & Booth, D. Intestinal stem cells protect their genome by selective segregation of template DNA strands. *J. Cell Sci.* **115**, 2381–2388 (2002).
20. Bjerknes, M. & Cheng, H. Gastrointestinal stem cells. II. Intestinal stem cells. *Am. J. Physiol. Gastrointest. Liver Physiol.* **289**, G381–G387 (2005).
21. Bjerknes, M. & Cheng, H. Intestinal epithelial stem cells and progenitors. *Methods Enzymol.* **419**, 337–383 (2006).
22. Wong, M.H., Saam, J.R., Stappenbeck, T.S., Rexer, C.H. & Gordon, J.I. Genetic mosaic analysis based on Cre recombinase and navigated laser capture microdissection. *Proc. Natl. Acad. Sci. USA* **97**, 12601–12606 (2000).
23. Clarke, M.F. & Fuller, M. Stem cells and cancer: two faces of Eve. *Cell* **124**, 1111–1115 (2006).
24. Harada, N. *et al.* Intestinal polyposis in mice with a dominant stable mutation of the β-catenin gene. *EMBO J.* **18**, 5931–5942 (1999).
25. Wu, S., Wu, Y. & Capecchi, M.R. Motoneurons and oligodendrocytes are sequentially generated from neural stem cells but do not appear to share common lineage-restricted progenitors *in vivo*. *Development* **133**, 581–590 (2006).
26. Barker, N. *et al.* Identification of stem cells in small intestine and colon by marker gene *Lgr5*. *Nature* **449**, 1003–1007 (2007).
27. Akasaka, T. *et al.* Mice doubly deficient for the Polycomb Group genes *Mel18* and *Bmi1* reveal synergy and requirement for maintenance but not initiation of *Hox* gene expression. *Development* **128**, 1587–1597 (2001).
28. Preston, S.L. *et al.* Bottom-up histogenesis of colorectal adenomas: origin in the monocryptal adenoma and initial expansion by crypt fission. *Cancer Res.* **63**, 3819–3825 (2003).
29. Shih, I.M. *et al.* Top-down morphogenesis of colorectal tumors. *Proc. Natl. Acad. Sci. USA* **98**, 2640–2645 (2001).